Journal of Cell Communication and Signaling (2023) 17:993–1008
https://doi.org/10.1007/s12079-023-00751-0

RESEARCH ARTICLE

MiR-218-5p promotes trophoblast infiltration and inhibits endoplasmic reticulum/oxidative stress by reducing UBE3A-mediated degradation of SATB1

Xiao Gu[1,2,3] · Xiaomei Sun[1,2] · Yanling Yu[2,4] · Lei Li[1,2,3,5]

Received: 21 June 2022 / Accepted: 10 April 2023 / Published online: 16 May 2023

Abstract

This research evaluated the effects of miR-218-5p on trophoblast infiltration and endoplasmic reticulum/oxidative stress during preeclampsia (PE). The expression of miR-218-5p and special AT-rich sequence binding protein 1 (SATB1) in placental tissues from 25 patients with PE and 25 normal pregnant subjects was determined using qRT-PCR and western blotting. Cell invasion and cell migration were detected by performing Transwell assays and scratch assays, respectively. MMP-2/9, TIMP1/2, HIF-1α, p-eIF2α, and ATF4 expression in cells was assessed through western blotting. Intracellular reactive oxygen species were detected using 2,7-dichlorodihydrofluorescein diacetate, and intracellular malondialdehyde and superoxide dismutase activities were determined with kits. Dual-luciferase and RNA pull-down assays were performed to verify the interaction between miR-218-5p and UBE3A. Co-immunoprecipitation and western blotting were used to detect the ubiquitination levels of SATB1. A rat model of PE was established, and an miR-218-5p agomir was injected into rat placental tissues. The pathological characteristics of placental tissues were detected via HE staining, and MMP-2/9, TIMP1/2, p-eIF2α, and ATF4 expression in rat placental tissues was determined through western blotting. MiR-218-5p and SATB1 were expressed at low levels, while UBE3A was highly expressed in the placental tissues of patients with PE. The transfection of an miR-218-5p mimic, UBE3A shRNA, or an SATB1 overexpression vector into HTR-8/SVneo cells promoted trophoblast infiltration and inhibited endoplasmic reticulum/oxidative stress. It was determined that UBE3A is a target of miR-218-5p; UBE3A induces ubiquitin-mediated degradation of SATB1. In PE model rats, miR-218-5p alleviated pathological features, promoted trophoblast infiltration, and inhibited endoplasmic reticulum/oxidative stress. MiR-218-5p targeted and negatively regulated UBE3A expression to inhibit ubiquitin-mediated SATB1 degradation, promote trophoblast infiltration, and inhibit endoplasmic reticulum/oxidative stress.

Keywords MiR-218-5p · UBE3A · SATB1 · Trophoblast infiltration · Ubiquitination

Co-first authors: Xiao Gu and Xiaomei Sun.

✉ Lei Li
lilei@sdfmu.edu.cn

[1] Department of Obstetrics and Gynecology, Shandong Provincial Hospital Affiliated to Shandong First Medical University, No. 324, Jingwuwei Seven Road, Jinan 250021, Shandong, People's Republic of China

[2] Department of Obstetrics and Gynecology, Shandong Provincial Hospital, Cheeloo College of Medicine, Shandong University, Jinan 250021, Shandong, People's Republic of China

[3] The Laboratory of Medical Science and Technology Innovation Center (Institute of Translational Medicine), Shandong First Medical University (Shandong Academy of Medical Sciences) of China, Jinan 250117, Shandong, People's Republic of China

[4] Department of Obstetrics and Gynecology, People's Hospital of Xiajin County, Dezhou 253299, Shandong, People's Republic of China

[5] The Laboratory of Placenta-Related Diseases, Key Laboratory of Birth Regulation and Control Technology of National Health and Family Planning Commission of China, Jinan 250025, Shandong, People's Republic of China

Introduction

Preeclampsia (PE) is a severe pregnancy complication that affects 5–7% of pregnant women worldwide and results in approximately 70,000 maternal and 500,000 fetal deaths per year (Jena et al. 2020). It is a dysfunction of placental trophoblast infiltration, which is caused by the immersion of trophoblasts in the shallow endometrial layer. PE is complicated by uterine vascular recasting disorders, thereby causing placental tissue ischemia, hypoxia, and a series of clinical manifestations (Lou et al. 2018; Yang et al. 2021). The pathogenesis of PE is considered to be associated with placental dysfunction induced by oxidative stress, inflammation, and endoplasmic reticulum stress (Ahmad et al. 2019; Aouache et al. 2018; Yang et al. 2020). Pathological research has shown that hypoxia, ischemia, and hypoperfusion in the uterus and placenta occur at high frequencies during placental vascular remodeling (Zou et al. 2018). Therefore, molecular mechanisms related to trophoblast infiltration and oxidative stress or endoplasmic reticulum stress in the pathogenesis of PE need to be investigated.

MicroRNAs (miRs) have been reported to participate in the development and progression of PE (Frazier et al. 2020; Liu et al. 2019; Zhang et al. 2020). Additionally, previous evidence has indicated that some miRs can ameliorate endoplasmic reticulum stress and prevent the inflammatory response, as well as oxidative stress (Tian et al. 2020; Yuan et al. 2020). A previous study found that the downregulation of miR-31 and miR-21 expression is related to PE (Dong et al. 2019). MiR-218 suppresses the invasion of trophoblast cells and is involved in the progression of PE (Fang et al. 2017). A recent study also reported an association between miR-218-5p and oxidative stress (Chen et al. 2021). Several studies have presented evidence indicating that special AT-rich sequence binding protein 1 (SATB1) is involved in the development of PE and is related to the migratory and invasive capabilities of trophoblasts and oxidative stress (Rao et al. 2018; Rao et al. 2019). UBE3A is an E3 ubiquitin ligase that specifically recognizes various substrates and mediates ubiquitination-associated degradation (Wang et al. 2019). Using the online database starBase (http://starbase.sysu.edu.cn/), we found that UBE3A is a target of miR-218-5p. Hence, in this study, we determined the correlations among miR-218-5p, UBE3A, and SATB1 and their effects on trophoblast infiltration and endoplasmic reticulum/oxidative stress in PE.

Materials and methods

Clinical subjects and tissue collection

Placental tissues were collected from 25 patients with PE and 25 normal pregnant subjects who received perinatal medical care at Shandong Provincial Hospital Affiliated to Shandong First Medical University. Written informed consent was acquired from the subjects or their families for the acquisition and use of all study samples. All study protocols were approved by the Ethics Committee of the Shandong Provincial Hospital Affiliated to Shandong First Medical University (approval number: 2019–238) and in accordance with the ethical principles of the "Declaration of Helsinki" for medical research on human subjects. Patients with renal disease, transient hypertension during pregnancy, gestational diabetes, spontaneous abortion, intrauterine fetal death, fetal chromosomal or congenital abnormalities, or pregnancy after treatment were excluded from this study. Placental tissues were collected within 1 h after cesarean section, and the collected tissues were immediately frozen and stored in liquid nitrogen for the subsequent extraction of RNA or protein. The diagnostic criteria for PE were as follows (Brkic et al. 2018): the patient had no pre-existing or chronic history of hypertension, but had a systolic blood pressure > 140 mmHg or a diastolic blood pressure > 90 mmHg at least twice after 20 weeks of pregnancy, accompanied by proteinuria (> 2 g every 24 h based on two samples collected > 4 h apart). Normal pregnant subjects match patients with PE in terms of age and gestational age. General data of patients with PE and normal pregnant subjects are shown in Table 1.

Cell culture and treatment

The human trophoblastic cell line HTR-8/SVneo was purchased from the ATCC (Manassas, VA, USA). Cells were cultured in DMEM (Gibco, Grand Island, NY, USA) containing 10% FBS, 1% penicillin, and 1% streptomycin and incubated in an incubator at 37 °C with 5% CO_2. An in vitro PE cell model was established by treating HTR-8/SVneo cells in the hypoxia–reoxygenation (H/R) mode, and HTR-8/SVneo cells were incubated at 37 °C for 8 h in a hypoxic chamber containing 2% oxygen and then incubated at 37 °C for 16 h in the presence of 20% oxygen. HTR-8/SVneo cells were transfected or co-transfected with a miR-218-5p mimic (50 nM, GenePharma, Shanghai, China), miR-218-5p inhibitor (50 nM, GenePharma, Shanghai, China), pcDNA3.1-UBE3A (2 μg, Jima Gene, Shanghai, China), sh-UBE3A (50 nM, GenePharma, Shanghai, China), pcDNA3.1-SATB1 (2 μg, GenePharma, Shanghai, China), sh-SATB1 (50 nM, GenePharma, Shanghai, China), or their corresponding negative controls. Transfection was performed using LipoFiter™ transfection reagent (HanBio, Shanghai, China) according to the transfection instructions. Three replicates were set up for transfection experiments, and induction was performed using H/R 24 h after transfection.

Table 1 General data of PE patients and normal pregnant subjects

	Control	PE	*P* value
N	25	25	
Gestational age (weeks)	36.51 ± 0.75	35.99 ± 0.68*	0.01325
Maternal age (years)	30.70 ± 1.65	29.87 ± 1.53	0.07189
Maternal weight (kg)	71.74 ± 1.34	71.71 ± 1.46	0.94217
Systolic BP (mmHg)	115.35 ± 0.97	146.27 ± 2.23***	5.14614E−48
Diastolic BP (mmHg)	75.63 ± 1.03	94.70 ± 1.63***	6.70022E−43
Proteinuria (g/24 h)	0	3.08 ± 0.36***	6.11249E−40
50 g GLU	7.26 ± 0.58	7.00 ± 0.45	0.08700
Baby weight (g)	3348.91 ± 37.88	2773.41 ± 23.84***	3.16449E−48

50 g GLU, 50 g oral glucose challenge test. *$P < 0.05$, ***$P < 0.001$, compared to control group

Animal experiment

All animal experiments were conducted with the approval of the Animal Care and Use Committee of the Shandong Provincial Hospital Affiliated to Shandong First Medical University (approval number: 2019–341). Sexually mature 24 female and 24 male Wistar rats (200–250 g, 8 weeks of age) were purchased from Shanghai Laboratory Animal Center, Chinese Academy of Sciences. All animals were housed under pathogen-free conditions, with a 12 h light/12 h dark cycle, temperature of 18–28 °C, humidity of 40–70%, and free access to food and water. The PE rat model was generated via the intraperitoneal injection of 50 mg/kg of the nitric oxide synthase inhibitor N(G)-nitro-L-arginine methyl ester (L-NAME, Beyotime, Shanghai, China) (Yan et al. 2014). The blood pressure of rats increased by 20 mmHg and was higher than 115 mmHg; combined with increased proteinuria, this indicated that the PE model was successfully established. Male and female rats were housed at a ratio of 1:1 and placed in separate, dedicated cages from 5 to 6 p.m.. The next day, sperm in the vaginal secretions of the female rats were observed, with vaginal plugs, through microscopy. If the test result was positive on that day, the day was recorded as day 0 of pregnancy. The female rats were divided into four groups from day 10 of pregnancy, with six rats in each group as follows: normal group (intraperitoneal injection of the same amount of saline from day 13 to day 20 of pregnancy), PE group (intraperitoneal injection of 50 mg/kg L-NAME every day from day 13 to day 20 of pregnancy and 20 μL of saline into the placenta from day 16 to day 19 of pregnancy), PE + miR-NC group (intraperitoneal injection of 50 mg/kg L-NAME every day from day 13 to day 20 of pregnancy, and injection of 20 μL containing 4 nmol miR-NC into the placenta from day 16 to day 19 of pregnancy), PE + miR-218-5p agomir group (intraperitoneal injection of 50 mg/kg L-NAME every day from day 13 to day 20 of pregnancy, and injection of 20 μL containing 4 nmol miR-218-5p agomir into the placenta from day 16 to day 19 of pregnancy). The rats were anesthetized with 3% pentobarbital sodium on day 21 of pregnancy, and the fetuses and placentas were obtained via Cesarean section. The umbilical cords connected to the fetuses were cut, and the placentas and fetuses were placed on a sterile gauze to dry the blood and amniotic fluid, respectively, and then placed on an analytical balance for weighing.

Quantitative reverse transcription PCR (qRT-PCR)

Total RNA was extracted using TRIZOL (Invitrogen, Carlsbad, CA, USA). Reverse transcription was performed using a reverse transcription kit (TaKaRa, Tokyo, Japan), and all procedures were conducted as per the instructions of the kit. The expression of genes was detected using a LightCycler480 (Roche, Indianapolis, IN, USA) via quantitative fluorescence PCR, and the reaction conditions were in accordance with the operating instructions of the quantitative fluorescence PCR kit (SYBR Green Mix, Roche Diagnostics, Indianapolis, IN). Thermal cycling parameters were as follows: 95 °C for 10 s, followed by 45 cycles of 95 °C for 5 s, 60 °C for 10 s, and 72 °C for 10 s; the final extension was at 72 °C for 5 min. Each reaction in the quantitative PCR was repeated thrice, with U6 as the miRNA internal reference and *GAPDH* as the mRNA internal reference. Data were analyzed using the $2^{-\Delta\Delta Ct}$ method, with ΔΔCt = experimental group (Ct target gene − Ct internal reference) − control group (Ct target gene − Ct internal reference). The amplification primer sequences for each gene and its internal reference are detailed in Table 2.

Western blotting

Cells were lysed using RIPA lysis solution (Beyotime, Shanghai, China) to obtain protein samples. After measuring the protein concentration with a BCA kit (Beyotime, Shanghai, China), the corresponding volume of the protein sample was taken and added to sample buffer (Beyotime,

Table 2 Primer sequences

Name of primer	Sequences
miR-218-5p-F	TTGTGCTTGATCTAA
miR-218-5p-R	CAGTGCGTGTCGTGGAGT
U6-F	CTCGCTTCGGCAGCACA
U6-R	AACGCTTCACGAATTTGCGT
UBE3A-F	CTCGGGGTGACTACAGGAGA
UBE3A-R	GGCAGAGGTGAAGCGTAAGT
SATB1-F	GGCAACTGGTAACCACCTCA
SATB1-R	GGACCCTTCGGATCACTCAC
GAPDH-F	AATGGGCAGCCGTTAGGAAA
GAPDH-R	GCGCCCAATACGACCAAATC

F forward, *R* reverse

Shanghai, China), mixed well, and heated in a boiling water bath for 3 min to denature the proteins. Electrophoresis was performed at 80 V for 30 min, and after bromophenol blue entered the separation gel, samples were electrophoresed for 1–2 h at 120 V. Membrane transfer was performed in an ice bath with a current of 300 mA for 60 min. After membrane transfer, the membrane was rinsed in the washing solution for 1–2 min and then placed in the blocking solution at room temperature for 60 min or blocked at 4 °C overnight. Primary antibodies [UBE3A (ab272168, 1:1000), SATB1 (ab109122, 1:1000), MMP2 (ab92536, 1:1000), MMP9 (ab76003, 1:1000), TIMP1 (ab211926, 1:1000), TIMP2 (ab180630, 1:500), ATF4 (ab184909, 1:1000), HIF-1α (ab179483, 1:1000), GAPDH (ab8245, 1:2000, Abcam, Cambridge, MA, USA), p-eIF2α (3398, 1:1000), eIF2α (5324, 1:1000, Cell Signaling, Boston, USA)] were incubated with the blots on a shaker for 1 h at room temperature, with the membranes then washed three times (10 min per time). Secondary antibodies were added, and the blots were incubated for 1 h at room temperature, with the membranes then washed three times for 10 min/time. After pipetting the developer onto the membrane, a chemiluminescence imaging system (Bio-Rad, Hercules, CA, USA) was used for protein detection.

Dual-luciferase reporter assay

The site of miR-218-5p binding to UBE3A was predicted using the online database starBase (http://starbase.sysu.edu.cn/). According to the predicted results, wild-type and mutant sequences of the binding site (mut-UBE3A and wt-UBE3A, respectively) were designed and synthesized. The wild-type and mutated sequences of the binding sites were inserted into the luciferase reporter vector (pGL3-Promoter, Promega, MADISON, WI, USA) and then co-transfected into HEK293T cells with the miR-218-5p mimic (50 nM) or miR-218-5p mimic negative control (50 nM, GenePharma). The binding of miR-218-5p to UBE3A was confirmed by measuring the luminescence intensity of each group using a dual-luciferase reporter assay kit (Promega, Madison, WI, USA) after transfection. The experimental groups used to test miR-218-5p binding to UBE3A were designed as follows, with three replicates per experiment: mimic + mut-UBE3A group, mimic + wt-UBE3A group, mimic NC + mut-UBE3A group, and mimic NC + wt-UBE3A group.

RNA pull-down assay

RNA pull-down assays were performed using the Pierce Magnetic RNA–Protein Pull-Down kit (Millipore, Billerica, MA, USA). Biotinylated UBE3A (Geneseed, Guangzhou, China) or biotinylated negative control (NC) was incubated with HTR-8/SVneo cell lysate for 2 h at 25 °C. The UBE3A/miR-218-5p complex was captured with streptavidin-labeled immunomagnetic beads for 1 h at 25 °C. The mixture was then cultured with proteinase K-containing buffer for 1 h at 25 °C, and the eluted complexes were assessed via qRT-PCR.

Co-immunoprecipitation (Co-IP)

Cells were lysed through the addition of precooled RIPA lysate and centrifuged at 14,000×*g* for 15 min at 4 °C, and the supernatant was transferred to a new centrifuge tube. The antibody (1 μg) [UBE3A (ab272168) or SATB1 (ab228772, Abcam, Cambridge, MA, USA)] was added to 1 mL of lysate, and IgG antibody was added to the NC group; furthermore, the antigen–antibody mixture was placed overnight at 4 °C or slowly shaken for 2 h at room temperature on a shaker. Protein A/G agarose beads (100 μL, prepared with PBS solution to a 50% concentration) were added to capture the antigen–antibody complex, and the antigen–antibody mixture was shaken slowly at 4 °C overnight or incubated at room temperature for 1 h. Transient centrifugation was performed at 14,000 rpm for 5 s; the supernatant was removed, and the bead-antigen/antibody mixture was collected. After washing three times with 800 μL of precooled RIPA buffer, the bead-antigen/antibody mixture was suspended in 60 μL of 2 × loading buffer and mixed by gently tapping. The loaded samples were boiled for 5 min and centrifuged at 14,000×*g*, and the remaining agarose beads were collected. The supernatant was electrophoresed and boiled again for 5 min before electrophoresis for denaturation, and UBE3A or SATB1 protein expression was detected by performing western blotting.

Ubiquitination assay

HEK293 cells were transfected with pcDNA3.1-UBE3A (GenePharma, Shanghai, China), Myc-SATB1 (Genomeditech, Shanghai, China), and HA-ubiquitin (Genomeditech,

Shanghai, China) using LipoFiter™ transfection reagent (HanBio, Shanghai, China), according to the transfection instructions. Cells were treated with 20 μM of the proteasome inhibitor MG132 for 6 h, washed twice with chilled PBS, and then lysed with RIPA lysis buffer. Cytosolic proteins were obtained via centrifugation of the lysate and incubated overnight with the anti-SATB1 antibody (ab228772, Abcam, Cambridge, MA, USA). Protein A/G agarose beads (100 μL) were added to capture the antigen–antibody mixture, and the antigen–antibody mixture was shaken slowly and incubated for 4 h at 4 °C. After washing three times with lysis buffer and boiling in 2 × SDS loading buffer to release the proteins, immunoblotting was performed using an anti-ubiquitin antibody (ab134953, 1:2000, Abcam, Cambridge, MA, USA).

Transwell assay

After the chamber coated with Matrigel was removed from the freezer at − 20 °C and thawed at room temperature, 0.5 mL of serum-free culture medium was added to the transwell chambers (Coring, New York, USA) and 24-well plates, which were then placed at 37 °C and cultured in 5% CO_2 for 2 h, with all culture medium removed. Cells in the logarithmic growth phase were collected and prepared as single-cell suspensions and seeded evenly into a six-well plate. Three replicate wells were prepared for each group, with cells incubated in a 37 °C incubator with 5% CO_2. When the cell confluence reached 70–90%, the cells in each group were treated according to the experimental grouping, and cells were cultured for 24 h at 37 °C in an incubator with 5% CO_2. The cells in each group were digested with trypsin, collected, washed twice with PBS, and resuspended in serum-free DMEM, with the cell concentration adjusted accordingly. Culture medium with 10% FBS (600 μL) was added to the lower chamber, and 100 μL of the cell suspension was added to the upper chamber and cultured in an incubator with 5% CO_2 at 37 °C for 24 h. The chambers were taken out, and the supernatant was discarded. The residual cells in the inner side of the upper chamber that failed to pass through the membrane were wiped with a cotton swab. Paraformaldehyde (4%) was added to fix the penetrating cells on the outer side of chamber for 20 min. Wright–Giemsa staining was performed, and the numbers of invading cells in five fields were counted randomly using a high-power lens, which was followed by capturing images and recording.

Scratch assay

Cells in the logarithmic growth phase were collected, prepared as single-cell suspensions, and seeded into a six-well plate. After 24 h, the cells in each group were treated according to the groups and cultured in a 37 °C, 5% CO_2 incubator for 24 h. A sterile tip (100 μL) was used to scratch the six-well plate. The culture medium in the six-well plate was discarded, and cells were washed twice with PBS, followed by the addition of serum-free culture medium to continue the culture. Cells were observed and photographed, and the scratch area at 0 h was considered the control. The six-well plate was further cultured in an incubator with 5% CO_2 at 37 °C for 24 h, with cell migration observed and photographed.

Reactive oxygen species determination

Intracellular reactive oxygen species (ROS) levels were assessed using the fluorescent reagent 2,7-dichlorodihydrofluorescein diacetate (DCFH-DA; Merck, Shanghai, China), according to the instructions. Cells were seeded into 96-well plates with 5000 cells per well and incubated with 10 μM DCFH-DA for 30 min at 37 °C. At the end of incubation, cells were washed thrice with PBS to remove free DCFH-DA molecules. The fluorescence intensity of cells in each well was measured using a SYNERGY microplate reader (BioTek, Winooski, VT, USA) at a wavelength of 530 nm.

Determination of malondialdehyde and superoxide dismutase activities

The activities of malondialdehyde (MDA) and superoxide dismutase (SOD) in cells were detected with MDA and SOD kits (Sigma-Aldrich, Merck KGaA, Darmstadt, Germany), respectively, as per the manufacturer's instructions.

Determination of systolic blood pressure and 24-h urine protein in rats

The blood pressure of rats was measured using the tail-cuff artery pressure method. The systolic blood pressure of the tail artery in pregnant rats on days 10, 13, 16, and 19 of pregnancy was measured using a rat tail artery pressure detector (Tensys (R) Medical Inc., San Diego, CA, USA), with the mean value taken after three pressure measurements over a short period. Twenty-four-hour urine was collected on days 10, 13, 16, and 19 of pregnancy from pregnant rats with free access to diet and water. The urinary protein content was measured at the Nephrology Department of the local hospital.

Hematoxylin and eosin staining

Placental tissues were fixed in 10% neutral buffered formalin (Solarbio Biotechnology Co., Ltd., Beijing, China) for 1 day, dehydrated, embedded in paraffin, and cut into 5 μm

sections. Paraffin sections were deparaffinized with xylene, hydrated with graded ethanol, and stained with hematoxylin for 5 min; then, excess dye was washed off. Cell staining was differentiated using ethanol hydrochloride for 30 s, and samples were stained with eosin for 2 min, routinely dehydrated, cleared, mounted, observed under a microscope, and photographed.

Statistical analysis

Statistical analysis was performed with GraphPad Prism7 software. All data were presented as the mean ± standard deviation (mean ± SD). T-tests were used for comparisons between groups; a one-way analysis of variance test was used for comparisons among multiple groups, and Tukey's multiple comparisons test was used for post-hoc multiple comparisons. $P < 0.05$ was regarded as statistically significant.

Results

MiR-218-5p and SATB1 are expressed at low levels in placental tissues of patients with PE

Placental tissues were collected from 25 patients with PE and 25 normal pregnant subjects, and the expression of miR-218-5p and SATB1 in these tissues was detected via qRT-PCR or western blotting. qRT-PCR showed that the expression of miR-218-5p in placental tissues of patients with PE was markedly lower than that in normal pregnant subjects (Fig. 1A, $P < 0.01$); the expression of SATB1 protein in placental tissues of patients with PE was also markedly decreased compared with that in normal pregnant subjects (Fig. 1B, $P < 0.01$). These results indicated that miR-218-5p and SATB1 are expressed at low levels in placental tissues from patients with PE.

MiR-218-5p promotes trophoblast infiltration and inhibits endoplasmic reticulum/oxidative stress under hypoxia–reoxygenation conditions

The human trophoblastic cell line HTR-8/SVneo was treated in the hypoxia–reoxygenation (H/R) mode to establish an in vitro PE cell model. HTR-8/SVneo cells were transfected with a miR-218-5p mimic/inhibitor followed by H/R treatment. qRT-PCR and western blot results illustrated that the expression levels of miR-218-5p and SATB1 were significantly decreased in HTR-8/SVneo cells of the H/R group compared to those in the control group (Fig. 2A–B, $P < 0.05$). However, the expression of miR-218-5p and SATB1 was significantly downregulated after transfection with a miR-218-5p inhibitor, whereas the expression of miR-218-5p and SATB1 was significantly upregulated after transfection with a miR-218-5p mimic (Fig. 2A–B, $P < 0.05$). Transwell and scratch assays showed that the invasion and migration of HTR-8/SVneo cells were decreased in the H/R group relative to that in the control group (Fig. 2C–D, $P < 0.01$) and further significantly decreased after transfection with the miR-218-5p inhibitor. However, they were significantly enhanced after transfection with the miR-218-5p mimic (Fig. 2C–D, $P < 0.05$). Western blotting was performed to determine the expression of HIF-1α and the trophoblast infiltration-related proteins, MMP-2/9 and TIMP1/2. Compared with that in the control group, the expression of MMP2/9 was significantly downregulated, and the expression of TIMP1/2 and HIF-1α was significantly upregulated in HTR-8/SVneo cells of the H/R group. Moreover, the expression of MMP2/9 was further downregulated and that of TIMP1/2 was further upregulated in HTR-8/SVneo cells after transfection with the miR-218-5p mimic inhibitor. In contrast, the expression levels of MMP2/9 were increased and those of TIMP1/2 were decreased after transfection with the miR-218-5p mimic (Fig. 2E, $P < 0.05$). Intracellular ROS levels were measured using DCFH-DA, and MDA and SOD levels were detected using kits; results showed

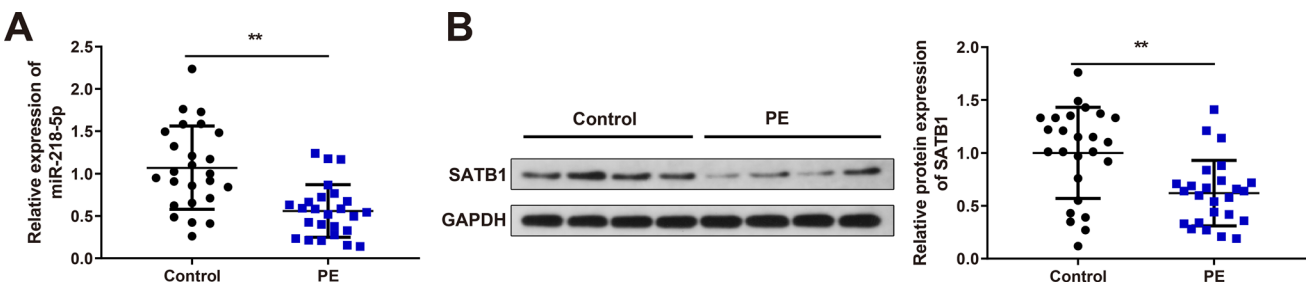

Fig. 1 Low miR-218-5p and SATB1 expressions in placental tissues from PE patients. Placental tissues were collected from 25 PE patients and 25 normal pregnant subjects. **A** miR-218-5p expression in placental tissues from PE patients and normal pregnant subjects detected by qRT-PCR; **B** SATB1 expression in placental tissues from PE patients and normal pregnant subjects measured by western blotting. $^{**}P < 0.01$, compared to the control group

that intracellular ROS and MDA levels were significantly increased and SOD levels were significantly decreased in HTR-8/SVneo cells of the H/R group compared with those in the control group. Intracellular ROS and MDA levels were further enhanced and SOD levels were further decreased in HTR-8/SVneo cells after transfection with the miR-218-5p inhibitor, but intracellular ROS and MDA levels were markedly reduced and SOD levels were markedly elevated after transfection with the miR-218-5p mimic (Fig. 2F–I, $P < 0.05$). Western blotting was conducted to detect the phosphorylation level of the endoplasmic reticulum stress-related protein eIF2α and expression of ATF4. Compared with that in the control group, the expression of p-eIF2α and ATF4 was significantly downregulated in HTR-8/SVneo cells of the H/R group, which was further reduced after transfection with the miR-218-5p inhibitor; however, the expression of p-eIF2α and ATF4 was markedly increased after transfection with the miR-218-5p mimic (Fig. 2J–L, $P < 0.05$). These findings suggest that miR-218-5p promoted trophoblast infiltration and inhibited endoplasmic reticulum/oxidative stress under H/R conditions.

UBE3A is a target gene of miR-218-5p

Based on the online database starBase (http://starbase.sysu.edu.cn/), UBE3A was predicted to have a binding site for miR-218-5p, and wild-type and mutant plasmids containing the 3′UTR region of UBE3A were constructed for dual-luciferase reporter assays (Fig. 3A). The results of the luciferase reporter assay to detect miR-218-5p binding to UBE3A showed that luciferase activity was markedly reduced in the mimic + wt-UBE3A group (Fig. 3B, $P < 0.01$). RNA pull-down analysis further indicated that endogenous miR-218-5p could be pulled down by the UBE3A biotinylated probe (Fig. 3C, $P < 0.05$). The expression of UBE3A in placental tissues of patients with PE and normal pregnant subjects, as well as in HTR-8/SVneo cells treated with H/R, was determined via qRT-PCR and western blotting. The findings demonstrated that UBE3A expression in placental tissues of patients with PE was markedly higher than that in normal pregnant subjects (Fig. 3D–E, $P < 0.01$). Moreover, UBE3A expression in HTR-8/SVneo cells treated with H/R was markedly higher than that in the control group (Fig. 3F–G, $P < 0.01$). HTR-8/SVneo cells were then exposed to H/R after transfection with the miR-218-5p mimic/inhibitor, and qRT-PCR and western blotting results showed that UBE3A expression was markedly upregulated in HTR-8/SVneo cells after transfection with the miR-218-5p inhibitor, but markedly decreased in HTR-8/SVneo cells after transfection with the miR-218-5p mimic (Fig. 3H–I, $P < 0.05$). These data indicated that UBE3A is a target gene of miR-218-5p.

UBE3A reverses the effects of miR-218-5p on trophoblast infiltration and endoplasmic reticulum/oxidative stress

We proceeded to investigate whether miR-218-5p would affect SATB1 expression by targeting UBE3A. After the co-transfection of the miR-218-5p mimic and pcDNA3.1-UBE3A or miR-218-5p inhibitor and sh-UBE3A into HTR-8/SVneo cells and exposure to H/R, UBE3A expression was markedly higher and SATB1 expression was significantly lower in the miR-218-5p mimic + pcDNA3.1-UBE3A group than in the miR-218-5p mimic group. Furthermore, UBE3A expression was markedly lower and SATB1 expression was markedly higher in the miR-218-5p inhibitor + sh-UBE3A group than in the miR-218-5p inhibitor group (Fig. 4A–B, $P < 0.05$). Transwell and scratch assays revealed that the overexpression of UBE3A could inhibit the promoting effect of the miR-218-5p mimic on trophoblast invasion and migration, whereas the knockdown of UBE3A could reverse the inhibitory effect of the miR-218-5p inhibitor on trophoblast invasion and migration (Fig. 4C–D, $P < 0.05$). We then showed that overexpression or knockdown of UBE3A could reverse the effect of miR-218-5p mimic or inhibitor on MMP-2/9 and TIMP1/2 expression in trophoblasts (Fig. 4E, $P < 0.05$). Intracellular ROS levels were measured using DCFH-DA, and MDA and SOD levels were determined using kits; the results showed that the overexpression of UBE3A could reverse the inhibitory effect of the miR-218-5p mimic on oxidative stress levels in trophoblasts, and the knockdown of UBE3A could reverse the promoting effect of the miR-218-5p inhibitor on oxidative stress levels in trophoblasts (Fig. 4F–I, $P < 0.05$). We then showed that the overexpression of UBE3A could reverse the promoting effect of the miR-218-5p mimic on p-eIF2α and ATF4 expression in trophoblasts, and the knockdown of UBE3A could reverse the inhibitory effect of the miR-218-5p inhibitor on p-eIF2α and ATF4 expression in trophoblasts (Fig. 4J–L, $P < 0.05$). These results indicated that UBE3A could reverse the effects of miR-218-5p on trophoblast infiltration and endoplasmic reticulum/oxidative stress.

UBE3A promotes SATB1 ubiquitination

UBE3A is an E3 ubiquitin ligase that specifically recognizes various substrates and mediates ubiquitination-mediated degradation (Wang et al. 2019). The expression of UBE3A was upregulated, whereas that of SATB1 was downregulated in PE, and miR-218-5p was found to target UBE3A and participate in the regulation of SATB1 expression. Thus, we speculated that UBE3A might be involved in the ubiquitin-mediated degradation of SATB1. qRT-PCR and western blotting results indicated that the overexpression of

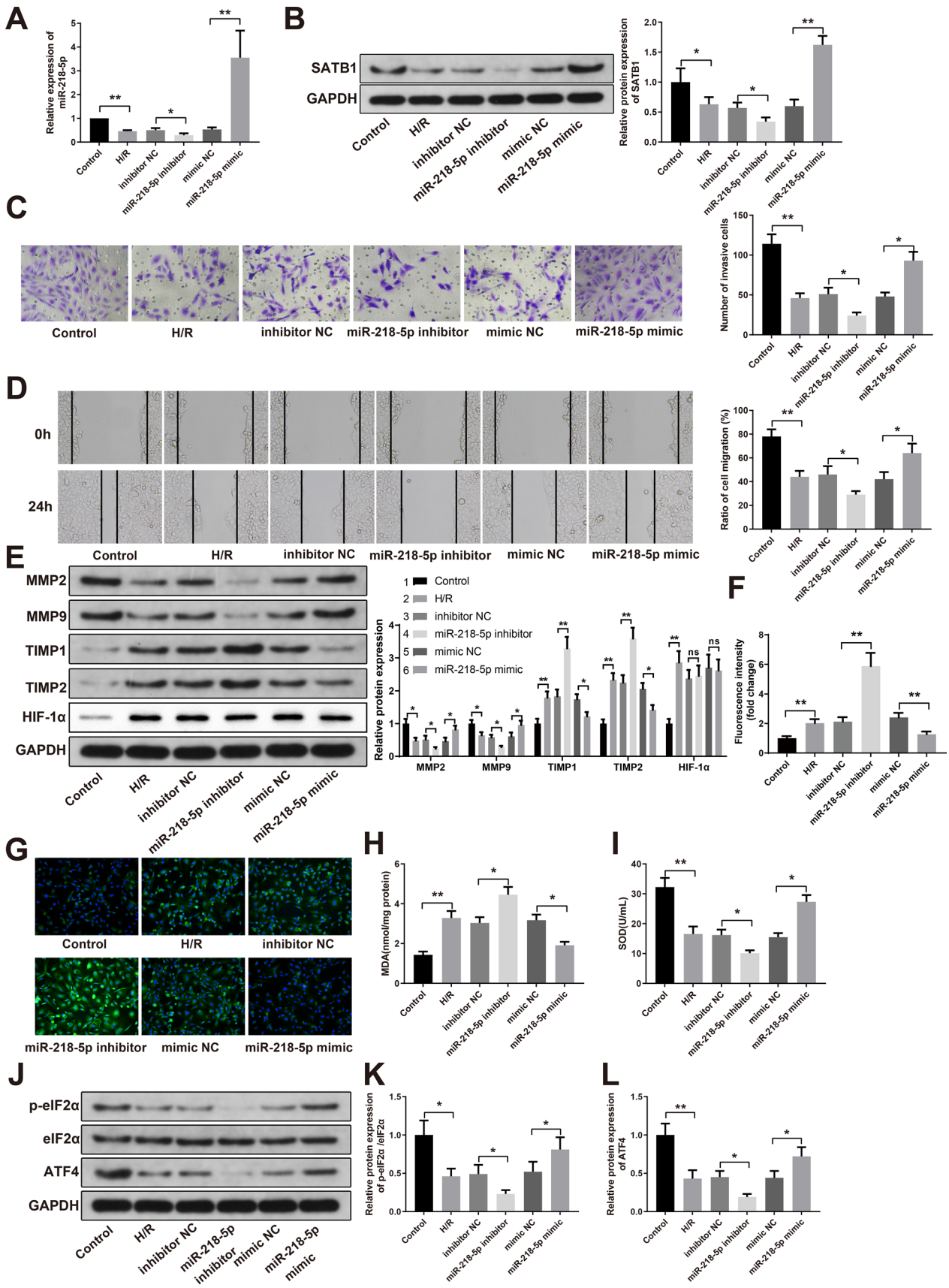
A
Relative expression of miR-218-5p
Control
H/R
inhibitor NC
miR-218-5p inhibitor
mimic NC
miR-218-5p mimic
B
SATB1
GAPDH
Relative protein expression of SATB1
C
Number of invasive cells
D
0h
24h
Ratio of cell migration (%)
E
MMP2
MMP9
TIMP1
TIMP2
HIF-1α
GAPDH
Relative protein expression
F
Fluorescence intensity (fold change)
G
H
MDA(nmol/mg protein)
I
SOD(U/mL)
J
p-eIF2α
eIF2α
ATF4
GAPDH
K
Relative protein expression of p-eIF2α /eIF2α
L
Relative protein expression of ATF4

◂**Fig. 2** MiR-218-5p promoted trophoblast infiltration and inhibited endoplasmic reticulum/oxidative stress in H/R condition. The human trophoblastic cell line HTR-8/SVneo was treated with H/R mode to establish an in vitro PE cell model, and HTR-8/SVneo cells were transfected with miR-218-5p mimic or miR-218-5p inhibitor followed by H/R treatment. **A** the expression of miR-218-5p in HTR-8/SVneo cells detected by qRT-PCR; **B** the expression of SATB1 in HTR-8/SVneo cells measured by western blotting; **C** cell invasion detected by Transwell assay; **D** cell migration tested by scratch assay; **E** the expressions of MMP-2/9, TIMP1/2, and HIF-1α in HTR-8/SVneo cells measured by western blotting; **F**–**G**: intracellular ROS level detected by DCFH-DA; **H**–**I**: the contents of MDA and SOD in cells detected by kit; **J**–**L**: the phosphorylation level of eIF2α and the expression of ATF4 in HTR-8/SVneo cells detected by western blotting; $^{*}P<0.05$, $^{**}P<0.01$, $^{***}P<0.001$, n = 3, compared to the control group or inhibitor NC group or mimic NC group

UBE3A had no effect on the mRNA expression of *SATB1* (Fig. 5A) but definitely decreased the protein expression of SATB1 (Fig. 5B, $P<0.05$). The inhibitory effect of UBE3A on SATB1 protein was reversed by the proteasome inhibitor MG132 (Fig. 5B), which suggested that UBE3A might be involved in the ubiquitin-mediated degradation of SATB1. Co-IP was performed to detect the binding of UBE3A to SATB1, and the results showed that with a UBE3A antibody, SATB1 protein was enriched; meanwhile, a SATB1 antibody led to UBE3A protein enrichment (Fig. 5C). HEK293 cells were then transfected with Myc-SATB1, pcDNA3.1-UBE3A, and HA-ubiquitin and treated with the proteasome inhibitor MG132, and SATB1 ubiquitination was analyzed via Co-IP assays and western blotting. The results showed that ubiquitin molecules binding to SATB1 were markedly

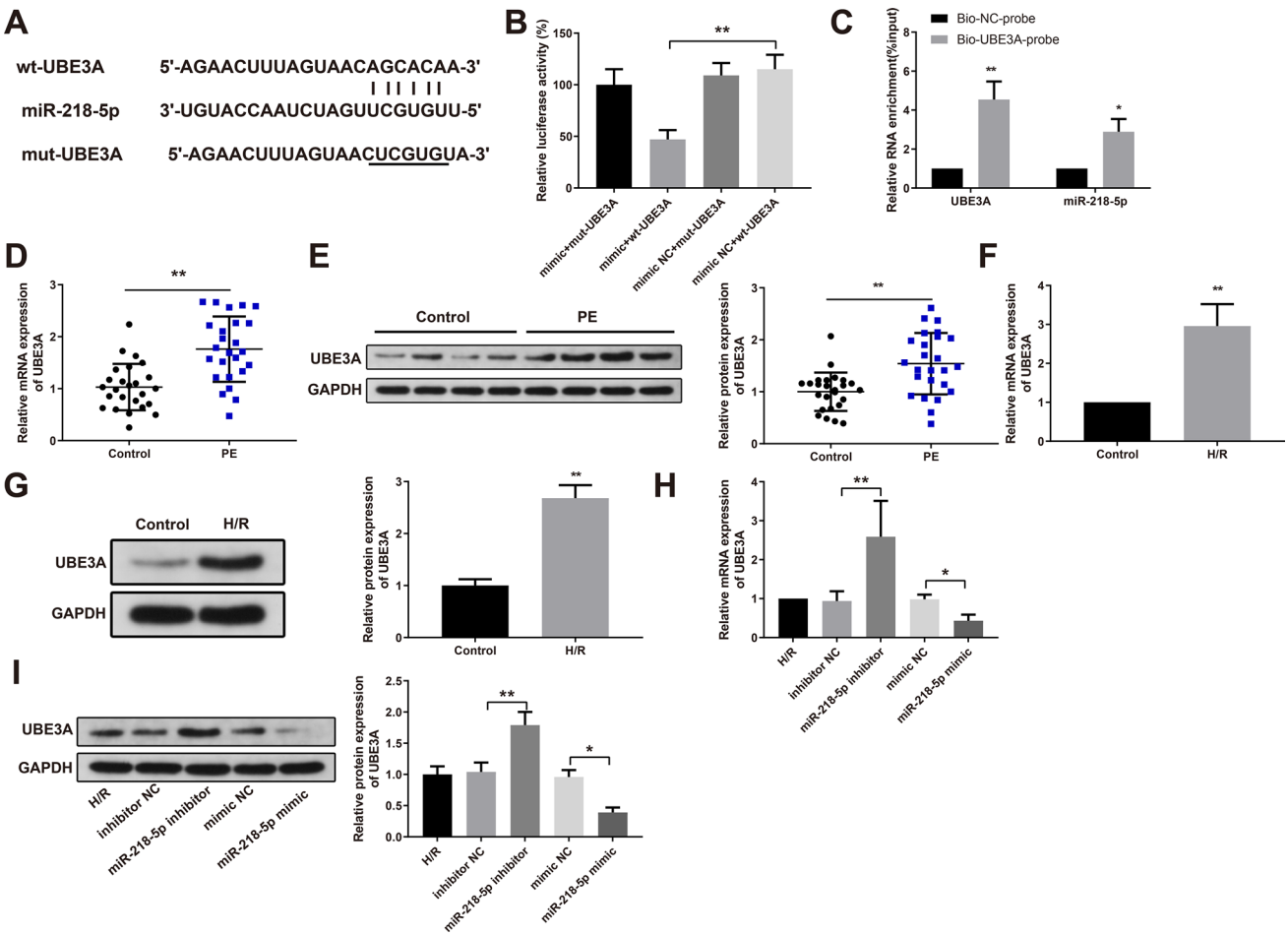

Fig. 3 UBE3A was a target gene of miR-218-5p. **A** the binding site of miR-218-5p and the 3'-UTR region of UBE3A; **B** the interaction between UBE3A and miR-218-5p confirmed by dual-luciferase reporter assay, $^{**}P<0.01$, compared to the mimic NC + wt-UBE3A group; **C** the interaction between UBE3A and miR-218-5p validated by RNA pull-down assay, $^{*}P<0.05$, $^{**}P<0.01$, compared to the bio-NC-probe group; **D**–**E** qRT-PCR and western blotting for the detection of UBE3A expression in placental tissue from PE patients and normal pregnant subjects, $^{**}P<0.01$, compared to the control group; **F**–**G**: the expression of UBE3A in HTR-8/SVneo cells treated with H/R detected by qRT-PCR and western blotting, $^{**}P<0.01$, compared to the control group. HTR-8/SVneo cells were exposed to H/R after transfection with miR-218-5p mimic or miR-218-5p inhibitor, **H**–**I**: the expression of UBE3A in HTR-8/SVneo cells detected by qRT-PCR and western blotting, $^{*}P<0.05$, $^{**}P<0.01$, compared to the inhibitor NC group or the mimic NC group

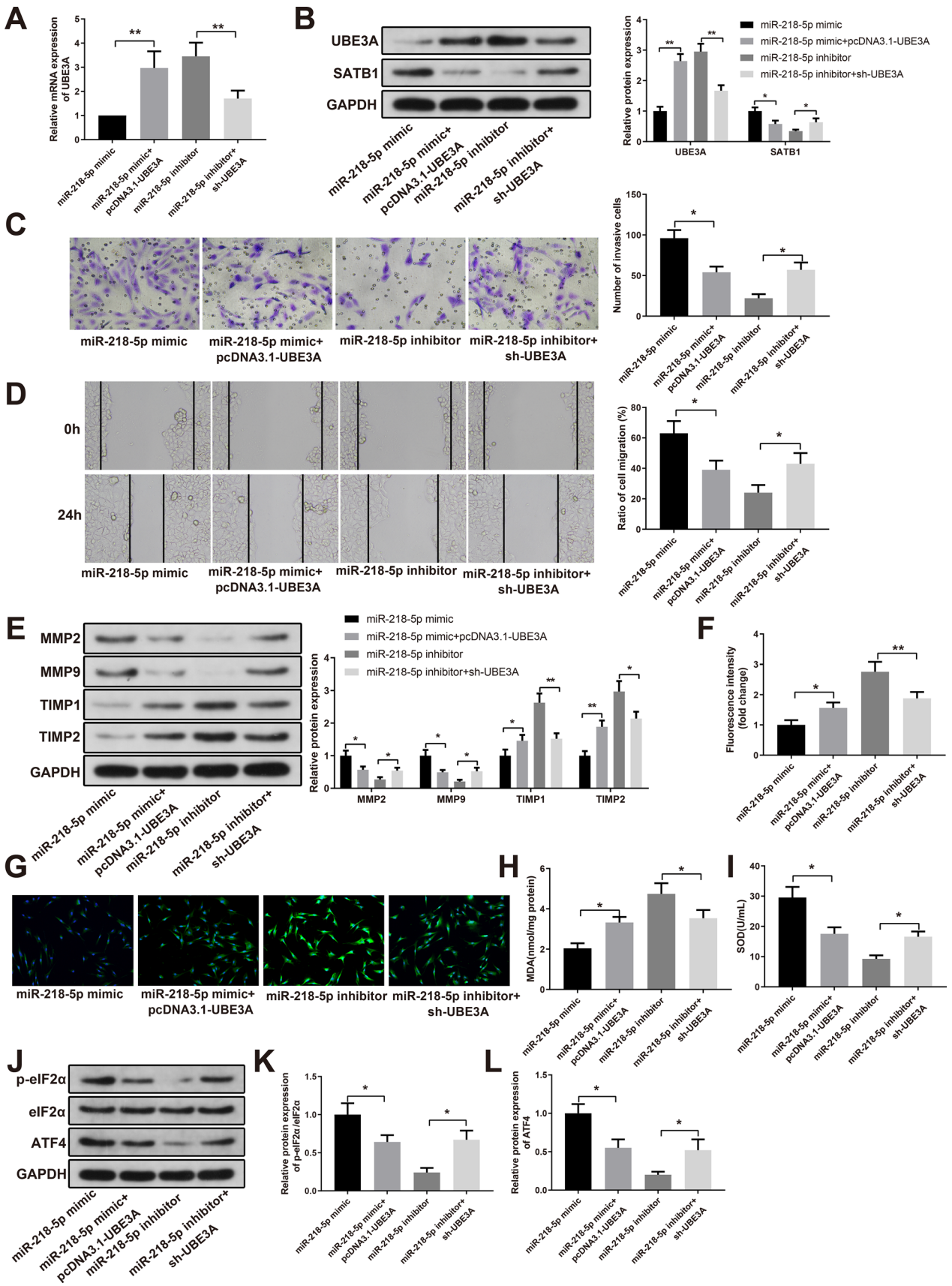
A
Relative mRNA expression of UBE3A
miR-218-5p mimic
miR-218-5p mimic+ pcDNA3.1-UBE3A
miR-218-5p inhibitor
miR-218-5p inhibitor+ sh-UBE3A
B
UBE3A
SATB1
GAPDH
Relative protein expression
miR-218-5p mimic
miR-218-5p mimic+pcDNA3.1-UBE3A
miR-218-5p inhibitor
miR-218-5p inhibitor+sh-UBE3A
C
Number of invasive cells
D
0h
24h
Ratio of cell migration (%)
E
MMP2
MMP9
TIMP1
TIMP2
GAPDH
Relative protein expression
F
Fluorescence intensity (fold change)
G
H
MDA(nmol/mg protein)
I
SOD(U/mL)
J
p-eIF2α
eIF2α
ATF4
GAPDH
K
Relative protein expression of p-eIF2α/eIF2α
L
Relative protein expression of ATF4

◂**Fig. 4** UBE3A reversed the effects of miR-218-5p on trophoblast infiltration and endoplasmic reticulum/oxidative stress. Exposure to H/R after co-transfection of miR-218-5p mimic and pcDNA3.1-UBE3A or miR-218-5p inhibitor and sh-UBE3A in HTR-8/SVneo cells, **A** the mRNA expression of UBE3A in HTR-8/SVneo cells detected by qRT-PCR; **B** the protein expressions of UBE3A and SATB1 in HTR-8/SVneo cells measured by western blotting; **C** cell invasion detected by Transwell assay; **D** cell migration detected by scratch assay; **E** the expressions of MMP-2/9 and TIMP1/2 in HTR-8/SVneo cells detected by western blot; **F–G** intracellular ROS level detected by DCFH-DA; **H–I** the contents of MDA and SOD in cells detected by kits; **J–L** the phosphorylation level of eIF2α and the expression of ATF4 in HTR-8/SVneo cells detected by western blotting; $^{*}P<0.05$, $^{**}P<0.01$, n = 3, compared to the miR-218-5p mimic group or the miR-218-5p inhibitor group

increased in cells overexpressing UBE3A compared to that in cells of the blank group, indicating that the overexpression of UBE3A could induce SATB1 ubiquitination (Fig. 5D). These observations demonstrated that UBE3A promotes SATB1 ubiquitination.

SATB1 reverses the effects of UBE3A on trophoblast infiltration and endoplasmic reticulum/oxidative stress

After the co-transfection of pcDNA3.1-UBE3A and pcDNA3.1-SATB1 or sh-UBE3A and sh-SATB1 into HTR-8/SVneo cells and exposure to H/R, western blotting results showed that the expression of SATB1 in the pcDNA3.1-UBE3A + pcDNA3.1-SATB1 group was markedly higher than that in the pcDNA3.1-UBE3A group and the expression of SATB1 in the sh-UBE3A + sh-SATB1 group was markedly lower than that in the sh-UBE3A group (Fig. 6A, $P<0.01$). Transwell and scratch assays suggested that SATB1 could reverse the inhibitory effect of UBE3A on trophoblast invasion and migration (Fig. 6B–C, $P<0.05$). We also found that SATB1 could reverse the effects of UBE3A on MMP-2/9 and TIMP1/2 expression in trophoblasts (Fig. 6D–E, $P<0.05$). Intracellular ROS levels were measured using DCFH-DA, and MDA and SOD levels were measured using kits; the results revealed that SATB1 could counteract the promoting effect of UBE3A on oxidative stress in trophoblasts (Fig. 6F–H, $P<0.05$). We further showed that SATB1 could reverse the inhibitory effects of UBE3A on p-eIF2α and ATF4 expression in trophoblasts (Fig. 6I–K, $P<0.05$). These observations provided evidence that SATB1 could reverse the effects of UBE3A on trophoblast infiltration and endoplasmic reticulum/oxidative stress.

Effects of miR-218-5p on PE in rats

A rat model of PE was generated via the intraperitoneal injection of L-NAME into Wistar rats, and an miR-218-5p agomir was injected into the placental tissues of rats to investigate the effects of miR-218-5p on PE-model rats. Systolic blood pressure on days 10, 13, 16, and 19 of pregnancy was measured, and 24 h urinary protein was tested in rats. The results showed that systolic blood pressure and 24 h urinary protein were markedly higher in the PE group than in the normal group and markedly lower in the PE + miR-218-5p agomir group than in the PE + miR-NC group (Fig. 7A-B, $P<0.05$). The neonatal rats and placenta were obtained from rats on day 21 of pregnancy as follows: 64 neonatal rats and placenta were collected from rats in the normal group; 62 neonatal rats and placenta were collected from rats in the PE group; 54 neonatal rats and placenta were collected from rats in the PE + miR-NC group; 51 neonatal rats and placenta were collected from rats in the PE + miR-218-5p agomir group (Fig. 7C). Fetal and placental weights were significantly lower in the PE group than in the normal group and markedly higher in the PE + miR-218-5p agomir group than in the PE + miR-NC group (Fig. 7D–E, $P<0.05$). We further showed that the expression of miR-218-5p and SATB1 was markedly reduced and that of UBE3A was markedly elevated in the placental tissues of rats in the PE group compared with the levels in the normal group. Moreover, the expression of miR-218-5p and SATB1 was markedly increased and that of UBE3A was decreased in the placental tissues of rats in the PE + miR-218-5p agomir group compared with the levels in the PE + miR-NC group (Fig. 7F–I, $P<0.05$). HE staining was performed to observe the pathological characteristics of placental tissues, and we found that the blood vessels in the placental villi of rats in the normal group were abundant, and the structure was clear. Furthermore, the trophoblasts of placental villi were mainly syncytiotrophoblasts, with few cytotrophoblasts. However, in the PE group, the number of placental villi was reduced, and these had a blurred and atrophic structure, with fibrinoid necrosis. Moreover, the syncytiotrophoblastic nodules of placental villi were increased, most of which were immature villi. Nonetheless, the pathological changes to placental tissues of rats were alleviated after the injection of miR-218-5p agomir (Fig. 7J). We also revealed that the expression of MMP2/9, p-eIF2α, and ATF4 was markedly decreased and that of TIMP1/2 was markedly increased in the placental tissues of rats in the PE group compared with the levels in the normal group. Furthermore, the expression of MMP2/9, p-eIF2α, and ATF4 was significantly elevated and that of TIMP1/2 was significantly decreased in the placental tissues of rats in the PE + miR-218-5p agomir group compared with the levels in the PE + miR-NC group (Fig. 7K–M, $P<0.05$). These observations suggested that miR-218-5p could alleviate pathological features, promote trophoblast infiltration, and inhibit endoplasmic reticulum/oxidative stress in PE-model rats.

Discussion

PE is characterized by placental ischemia and hypoxia and is mainly caused by insufficient trophoblast infiltration (Yang et al. 2021). The development of PE is commonly associated with dysregulated placental immunity, inflammation, and endoplasmic reticulum/oxidative stress. Accumulating evidence has revealed that miRs might improve oxidative stress and endoplasmic reticulum stress, in addition to enhancing trophoblast infiltration (Lv et al. 2019; Tian et al. 2020; Yuan et al. 2020). In this study, we identified a preliminary correlation among miR-218-5p, UBE3A, and SATB1, as well as their effects on trophoblast infiltration and endoplasmic reticulum/oxidative stress in PE.

First, we found that miR-218-5p and SATB1 were expressed at low levels in the placental tissues of patients with PE. Consistent with our findings, a previous study reported that miR-218-5p expression is significantly downregulated in PE placentas (Brkic et al. 2018). Additionally, previous data revealed low SATB1 expression in the placenta associated with PE and H/R-treated HTR8/SVneo cells (Rao et al. 2019). MiRs have been shown to regulate trophoblast behaviors, such as cell invasion, migration, and apoptosis. For example, Yan et al. found that miR-145-5p can enhance trophoblast cell proliferation and invasion by targeting FLT1 (Lv et al. 2019). Zhao et al. (2020) reported that the exosomal encapsulation of miR-125a-5p suppresses the migration and proliferation of trophoblasts by regulating VEGFA expression in PE. MiR-218-5p was also proven to promote the invasion of trophoblasts and endovascular extravillous trophoblast differentiation via the miR-218-5p-TGF-β2 pathway, and the low expression of miR-218-5p was found to contribute to the development of PE (Brkic et al. 2018). It was also reported that miR-218-5p inhibition can enhance oxidative stress in rheumatoid arthritis synovial fibroblasts (Chen et al. 2021). Consistent with

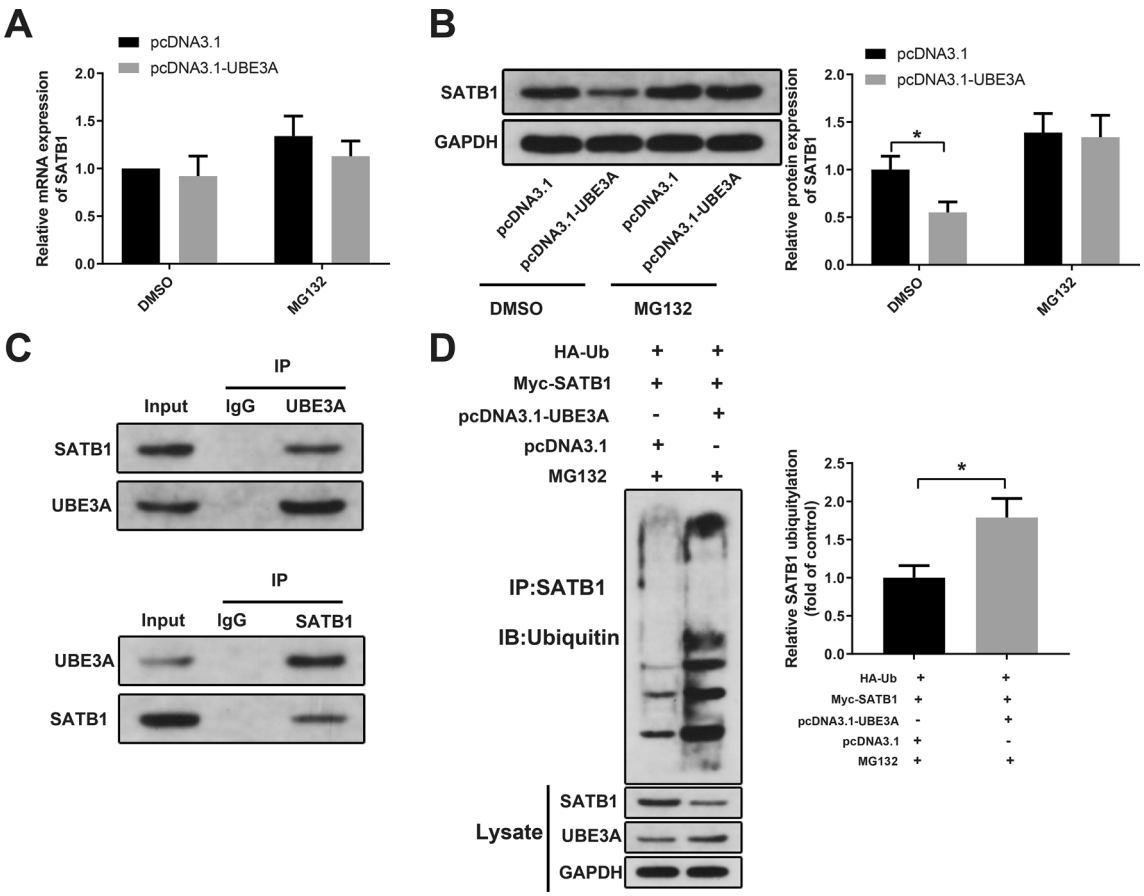

Fig. 5 UBE3A promoted SATB1 ubiquitination. HTR-8/SVneo cells transfected with pcDNA3.1-UBE3A for 24 h and then treated with proteasome inhibitor MG132 for 6 h. **A**: the effects of overexpression of UBE3A and treatment with proteasome inhibitor MG132 on the mRNA expression of SATB1 detected by qRT-PCR; **B** the effect of overexpression of UBE3A and treatment with proteasome inhibitor MG132 on SATB1 protein expression measured by western blotting, $^{*}P < 0.05$, compared to pcDNA3.1 group; **C** the binding of UBE3A to SATB1 in HTR-8/SVneo cells detected by Co-IP assay; D: HEK293 cells were transfected with Myc-SATB1, pcDNA3.1-UBE3A, HA-ubiquitin and treated with proteasome inhibitor MG132, and Co-IP assay and western blotting were used to detect ubiquitin protein expression for analyzing the effect of overexpression of UBE3A on SATB1 ubiquitination, $^{*}P < 0.05$, compared to the pcDNA3.1 group

prior findings, our experiments revealed that after transfection with the miR-218-5p mimic, MMP2/9 expression was markedly increased and TIMP1/2 expression was markedly decreased. Furthermore, intracellular ROS and MDA levels were markedly reduced, and SOD levels were markedly elevated, which suggests that miR-218-5p promotes trophoblast infiltration and inhibits endoplasmic reticulum/oxidative stress under H/R conditions. However, one study showed the upregulation of miR-218 expression in patients with PE (Fang et al. 2017). This variation could be caused by the differences in clinical samples, such as differences in the ethnicities of patients. Additionally, it is not clear whether miR-218-3p or miR-218-5p was detected in the aforementioned study. A larger number of clinical samples should be included to determine the expression of miR-218-5p and its relevance to clinical indices in patients with PE.

Using the online database starBase (http://starbase.sysu.edu.cn/), UBE3A was predicted to be a downstream gene of miR-218-5p. Previous evidence has demonstrated that the dysregulation of UBE3A contributes to transcriptional dysregulation associated with endoplasmic reticulum stress and inflammation, as a component of ubiquitination pathways (Torres-Odio et al. 2017). Related experiments proved that UBE3A could reverse the effects of miR-218-5p on trophoblast infiltration and endoplasmic reticulum/oxidative stress. UBE3A is an E3 ubiquitin ligase that specifically recognizes various substrates and mediates ubiquitination-associated degradation (Lopez et al. 2018; Wang et al. 2019). Our subsequent experiments showed that (i) the overexpression of UBE3A could markedly decrease the protein expression of SATB1, (ii) the inhibitory effect of UBE3A on SATB1 protein could be reversed by the proteasome inhibitor MG132,

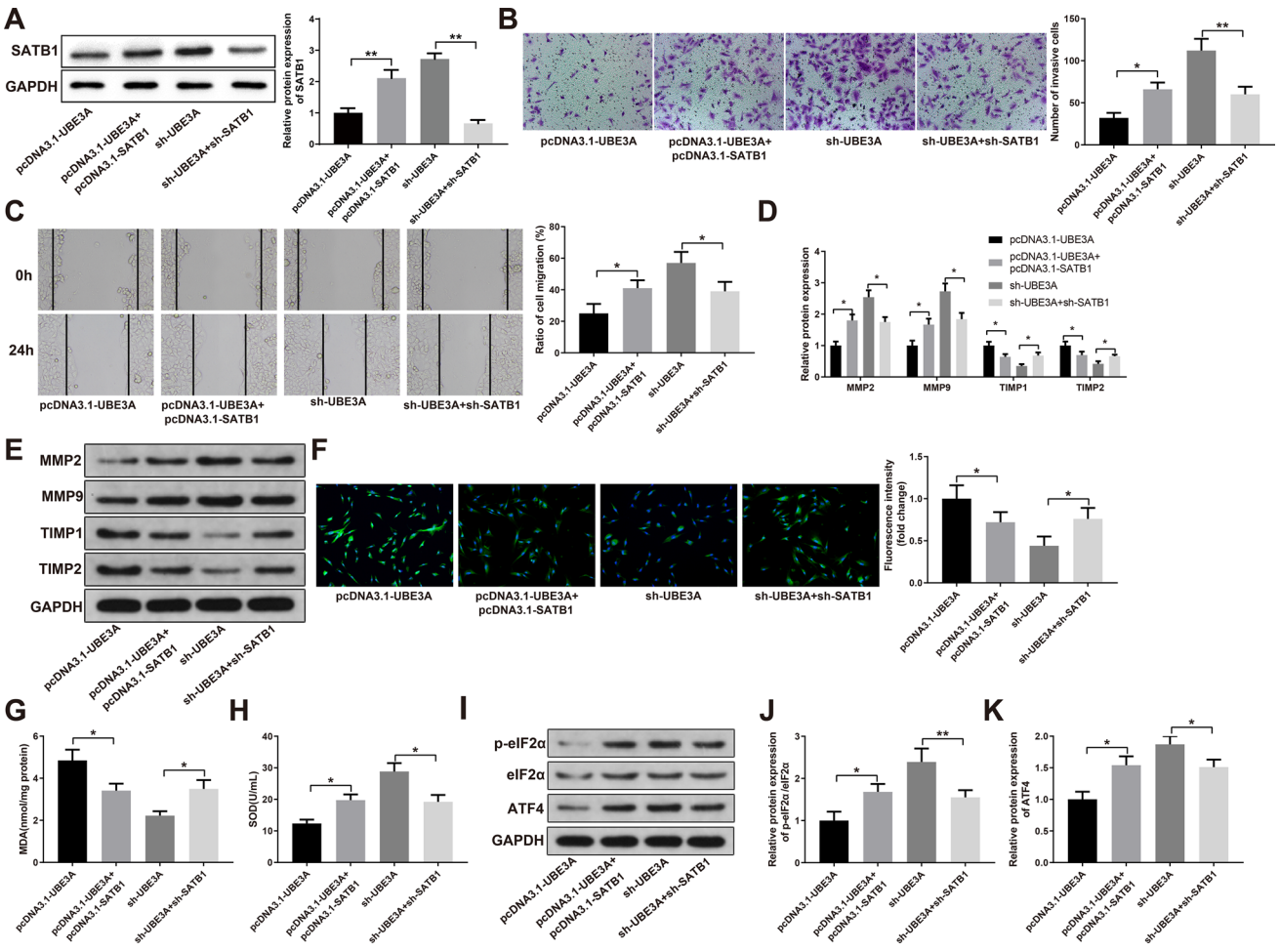

Fig. 6 SATB1 reversed the effects of UBE3A on trophoblast infiltration and endoplasmic reticulum/oxidative stress. Exposure to H/R after co-transfection of pcDNA3.1-UBE3A and pcDNA3.1-SATB1 or sh-UBE3A and sh-SATB1 in HTR-8/SVneo cells, **A** the expression of SATB1 in HTR-8/SVneo cells measured by western blotting; **B** cell invasion detected by Transwell assay; **C** cell migration detected by scratch assay; **D**–**E** the expressions of MMP-2/9 and TIMP1/2 in HTR-8/SVneo cells detected by western blot; **F** intracellular ROS level detected by DCFH-DA; **G**–**H** the contents of MDA and SOD in cells detected by kits; I–K: the phosphorylation level of eIF2α and the expression of ATF4 in HTR-8/SVneo cells detected by western blotting; $^{*}P<0.05$, $^{**}P<0.01$, n = 3, compared to the pcDNA3.1-UBE3A group or the sh-UBE3A group

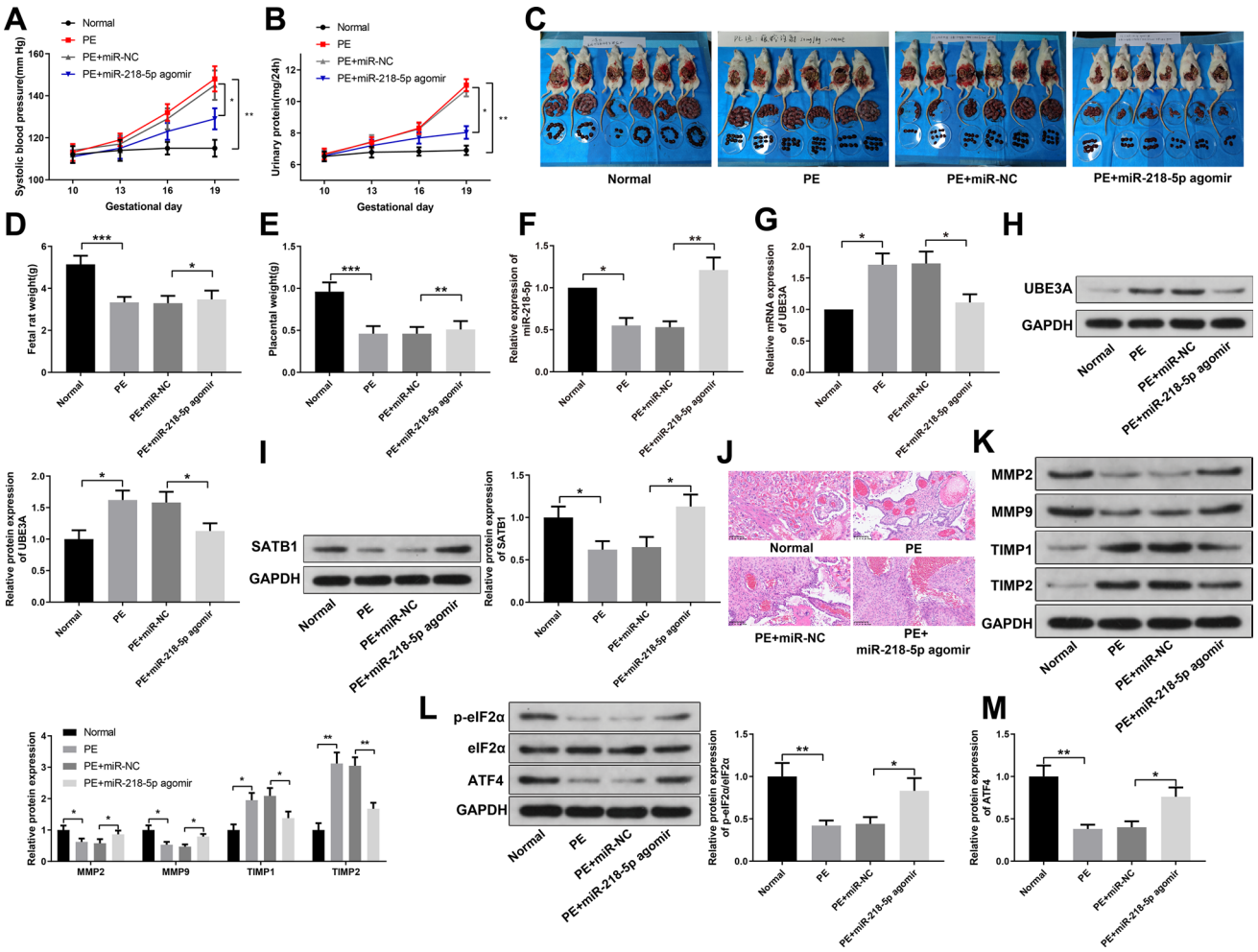

Fig. 7 Effects of miR-218-5p on PE rats. A rat model of PE was constructed by intraperitoneal injection of L-NAME in Wistar rats, and miR-218-5p agomir was injected into the placental tissue of rats. **A** systolic blood pressure was measured on Days 10, 13, 16, and 19 of pregnancy in rats, n = 6; **B** 24-h urinary protein was measured on Days 10, 13, 16, and 19 of pregnancy in rats, n = 6; **C** neonatal rats and placenta delivered by rats in each group; **D** measurement of fetal weight, Normal group: n = 64; PE group: n = 62; PE + miR-NC group: n = 54; PE + miR-218-5p agomir group: n = 51.; **E** measurement of placental weight in rats, Normal group: n = 64; PE group: n = 62; PE + miR-NC group: n = 54; PE + miR-218-5p agomir group: n = 51; **F–G** the expression of miR-218-5p and UBE3A in rat placenta detected by qRT-PCR, n = 6; **H–I** the expressions of UBE3A and SATB1 in rat placenta measured by western blotting; **J** pathological characteristics of placental tissue detected by HE staining, n = 6; L-M: the expressions of MMP-2/9 and TIMP1/2, p-eIF2α and ATF4 in rat placental tissues detected by western blotting, n = 6. $^{*}P < 0.05$, $^{**}P < 0.01$, n = 6, compared to the normal group or the PE + miR-NC group

and (iii) UBE3A promotes SATB1 ubiquitination. Consistent with our findings, SMURF2 was also found to be an E3 ubiquitin ligase, similar to UBE3A, that promotes SATB1 degradation by enhancing the ubiquitination of SATB1 (Yu et al. 2019). Previous evidence showed that oxidative stress leads to a decrease in the expression of SATB1, which was found to be related to impaired trophoblast functions (Rao et al. 2019). Rao et al. found that H/R-treated trophoblasts expressing lower SATB1 levels demonstrate a weaker invasion; however, an increase in the SATB1 level, with recombinant SATB1, could reverse these effects (Rao et al. 2018). Similar to the conclusions from previous studies, our study further found that SATB1 overexpression reverses the effects of UBE3A on trophoblast infiltration and endoplasmic reticulum/oxidative stress post-H/R treatment. Subsequent assays performed using a rat model of PE revealed that miR-218-5p could alleviate pathological features, promote trophoblast infiltration, and inhibit endoplasmic reticulum/oxidative stress in PE-model rats, which provides further support for the aforementioned findings using cells.

Based on the aforementioned findings, we concluded that miR-218-5p targets and negatively regulates UBE3A

expression, suppresses the ubiquitin-mediated degradation of SATB1, promotes trophoblast infiltration, and inhibits endoplasmic reticulum/oxidative stress. This is the first study to report the involvement of UBE3A in PE, which established a novel molecular axis linking miR-218-5p and SATB1 through UBE3A. The expression levels of these three molecules might thus be used as predictive and prognostic factors for PE. The miR-218-5p/UBE3A/SATB1 axis could also be a candidate target for molecule-based PE therapy.

Our study has some limitations. First, we did not explore the effects of miR-218-5p expression on inflammation, which is also an important process in PE. Second, many proteins other than SATB1 are involved in the progression of PE, and they might be linked to miR-218-5p expression, which should be explored in future studies. Third, exposure to endocrine-disrupting chemicals is a cause of abnormal placentation, increasing the risk of pregnancy disorders and predisposing the fetus to adverse health risks (Lorigo and Cairrao 2022; Yang et al. 2019). It might thus be interesting to investigate the influence of endocrine-disrupting chemicals on miR-218-5p in PE. In summary, our observations on miR-218-5p warrant further studies on other gestational disorders to support the contention that miR-218-5p might be a great candidate for the investigation of PE and associated therapeutics.

Acknowledgements We acknowledge and appreciate our colleagues for their valuable efforts and comments on this paper.

Author contributions LL conceived the ideas; designed the experiments. GX and SXM performed the experiments. GX; SXM and YYL analyzed the data. GX and SXM provided critical materials. GX; SXM and YYL wrote the manuscript. LL supervised the study. All the authors have read and approved the final version for publication.

Funding This work was supported by the Taishan Scholar Foundation of Shandong Province (Grant No. tsqn202103181), National Natural Science Foundation of China (Grant No. 81801473; 81971409; 81741037), and Jinan Science and Technology Bureau (Grant No. 201907011).

Declarations

Conflict of interest The authors have no competing interests to declare that are relevant to the content of this article.

Ethical approval Written informed consent was acquired from the subjects or their families for the acquisition and use of all study samples. All study protocols were approved by the Ethics Committee of the Shandong Provincial Hospital Affiliated to Shandong First Medical University (Approval Number: 2019–238) and in accordance with the ethical principles of the "Declaration of Helsinki" for medical research on human subjects. All animal experiments were conducted with the approval of the Animal Care and Use Committee of the Shandong Provincial Hospital Affiliated to Shandong First Medical University (Approval Number: 2019–341).

References

Ahmad IM, Zimmerman MC, Moore TA (2019) Oxidative stress in early pregnancy and the risk of preeclampsia. Pregnancy Hypertens 18:99–102. https://doi.org/10.1016/j.preghy.2019.09.014

Aouache R, Biquard L, Vaiman D, Miralles F (2018) Oxidative stress in preeclampsia and placental diseases. Int J Mol Sci. https://doi.org/10.3390/ijms19051496

Brkic J et al (2018) MicroRNA-218-5p promotes endovascular trophoblast differentiation and spiral artery remodeling. Mol Ther 26:2189–2205. https://doi.org/10.1016/j.ymthe.2018.07.009

Chen M, Li M, Zhang N, Sun W, Wang H, Wei W (2021) Mechanism of miR-218–5p in autophagy, apoptosis and oxidative stress in rheumatoid arthritis synovial fibroblasts is mediated by KLF9 and JAK/STAT3 pathways. J Investig Med. https://doi.org/10.1136/jim-2020-001437

Dong K, Zhang X, Ma L, Gao N, Tang H, Jian F, Ma Y (2019) Downregulations of circulating miR-31 and miR-21 are associated with preeclampsia. Pregnancy Hypertens 17:59–63. https://doi.org/10.1016/j.preghy.2019.05.013

Fang M et al (2017) Hypoxia-inducible microRNA-218 inhibits trophoblast invasion by targeting LASP1: implications for preeclampsia development. Int J Biochem Cell Biol 87:95–103. https://doi.org/10.1016/j.biocel.2017.04.005

Frazier S, McBride MW, Mulvana H, Graham D (2020) From animal models to patients: the role of placental microRNAs, miR-210, miR-126, and miR-148a/152 in preeclampsia. Clin Sci (lond) 134:1001–1025. https://doi.org/10.1042/CS20200023

Jena MK, Sharma NR, Petitt M, Maulik D, Nayak NR (2020) Pathogenesis of preeclampsia and therapeutic approaches targeting the placenta. Biomolecules. https://doi.org/10.3390/biom10060953

Liu S, Xie X, Lei H, Zou B, Xie L (2019) Identification of key circRNAs/lncRNAs/miRNAs/mRNAs and pathways in preeclampsia using bioinformatics analysis. Med Sci Monit 25:1679–1693. https://doi.org/10.12659/MSM.912801

Lopez SJ, Segal DJ, LaSalle JM (2018) UBE3A: an e3 ubiquitin ligase with genome-wide impact in neurodevelopmental disease. Front Mol Neurosci 11:476. https://doi.org/10.3389/fnmol.2018.00476

Lorigo M, Cairrao E (2022) Fetoplacental vasculature as a model to study human cardiovascular endocrine disruption. Mol Aspects Med 87:101054. https://doi.org/10.1016/j.mam.2021.101054

Lou CX, Zhou XT, Tian QC, Xie HQ, Zhang JY (2018) Low expression of microRNA-21 inhibits trophoblast cell infiltration through targeting PTEN. Eur Rev Med Pharmacol Sci 22:6181–6189. https://doi.org/10.26355/eurrev_201810_16023

Lv Y et al (2019) miR-145–5p promotes trophoblast cell growth and invasion by targeting FLT1. Life Sci 239:117008. https://doi.org/10.1016/j.lfs.2019.117008

Rao H, Bai Y, Zhang F, Li Q, Zhuang B, Luo X, Qi H (2019) The role of SATB1 in HTR8/SVneo cells and pathological mechanism of preeclampsia. J Matern Fetal Neonatal Med 32:2069–2078. https://doi.org/10.1080/14767058.2018.1425387

Rao H et al (2018) SATB1 downregulation induced by oxidative stress participates in trophoblast invasion by regulating beta-catenin. Biol Reprod 98:810–820. https://doi.org/10.1093/biolre/ioy033

Tian R, Wu B, Fu C, Guo K (2020) miR-137 prevents inflammatory response, oxidative stress, neuronal injury and cognitive impairment via blockade of Src-mediated MAPK signaling pathway in ischemic stroke. Aging (albany NY) 12:10873–10895. https://doi.org/10.18632/aging.103301

Torres-Odio S et al (2017) Progression of pathology in PINK1-deficient mouse brain from splicing via ubiquitination, ER stress, and

mitophagy changes to neuroinflammation. J Neuroinflammation 14:154. https://doi.org/10.1186/s12974-017-0928-0
Wang J et al (2019) UBE3A-mediated PTPA ubiquitination and degradation regulate PP2A activity and dendritic spine morphology. Proc Natl Acad Sci U S A 116:12500–12505. https://doi.org/10.1073/pnas.1820131116
Yan T et al (2014) Assessment of therapeutic efficacy of miR-126 with contrast-enhanced ultrasound in preeclampsia rats. Placenta 35:23–29. https://doi.org/10.1016/j.placenta.2013.10.017
Yang C, Song G, Lim W (2019) A mechanism for the effect of endocrine disrupting chemicals on placentation. Chemosphere 231:326–336. https://doi.org/10.1016/j.chemosphere.2019.05.133
Yang X, Chen D, He B, Cheng W (2021) NRP1 and MMP9 are dual targets of RNA-binding protein QKI5 to alter VEGF-R/ NRP1 signalling in trophoblasts in preeclampsia. J Cell Mol Med 25:5655–5670. https://doi.org/10.1111/jcmm.16580
Yang Y et al (2020) Endoplasmic reticulum stress may activate NLRP3 inflammasomes via TXNIP in preeclampsia. Cell Tissue Res 379:589–599. https://doi.org/10.1007/s00441-019-03104-9
Yu L et al (2019) Reversible regulation of SATB1 ubiquitination by USP47 and SMURF2 mediates colon cancer cell proliferation and tumor progression. Cancer Lett 448:40–51. https://doi.org/10.1016/j.canlet.2019.01.039
Yuan Q, Xu T, Chen Y, Qu W, Sun D, Liu X, Sun L (2020) MiR-185–5p ameliorates endoplasmic reticulum stress and renal fibrosis by downregulation of ATF6. Lab Invest 100:1436–1446. https://doi.org/10.1038/s41374-020-0447-y
Zhang H et al (2020) miR-30–5p-mediated ferroptosis of trophoblasts is implicated in the pathogenesis of preeclampsia. Redox Biol 29:101402. https://doi.org/10.1016/j.redox.2019.101402
Zhao X, Li Y, Chen S, Chen D, Shen H, Yang X, Cheng W (2020) Exosomal encapsulation of miR-125a-5p inhibited trophoblast cell migration and proliferation by regulating the expression of VEGFA in preeclampsia. Biochem Biophys Res Commun 525:646–653. https://doi.org/10.1016/j.bbrc.2020.02.137
Zou AX, Chen B, Li QX, Liang YC (2018) MiR-134 inhibits infiltration of trophoblast cells in placenta of patients with preeclampsia by decreasing ITGB1 expression. Eur Rev Med Pharmacol Sci 22:2199–2206. https://doi.org/10.26355/eurrev_201804_14804